


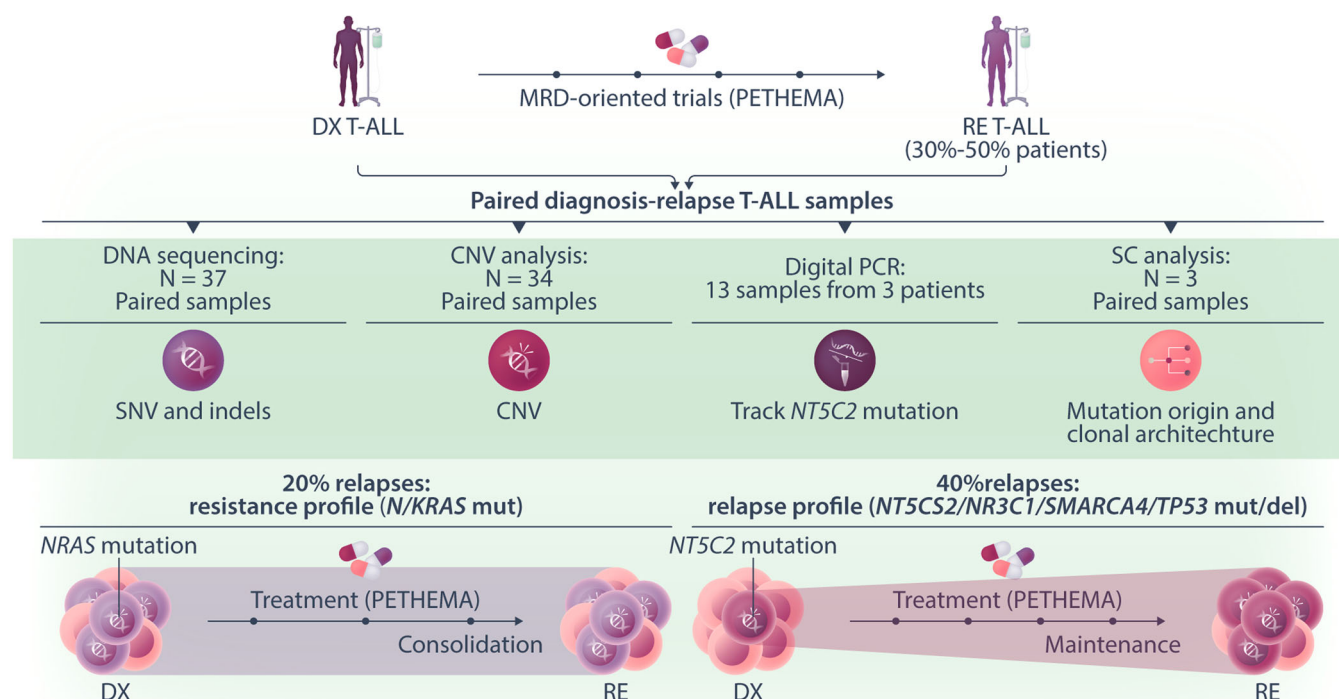


ARTICLE

Genetic evolution and relapse-associated mutations in adult T-cell acute lymphoblastic leukemia patients treated in PETHEMA trials

Celia González-Gil¹ | Thaysa Lopes^{1,^} | Mireia Morgades^{2,^} |
 Francisco Fuster-Tormo¹ | Pau Montesinos³  | Carlos Rodríguez Medina⁴ |
 Lourdes Hermosín⁵ | Teresa González-Martínez⁶ | María-Paz Queipo⁷ |
 José González-Campos⁸ | Pilar Martínez-Sánchez⁹ | Marina Díaz-Beya¹⁰ |
 Rosa Coll¹¹ | Clara Maluquer¹² | Lurdes Zamora^{1,2} | Teresa Artola¹³ |
 Ferran Vall-Llovera¹⁴ | Mar Tormo¹⁵ | Anna Torrent²  |
 Carolina Martínez-Laperche¹⁶ | Cristina Gil-Cortés¹⁷ | Pere Barba¹⁸ |
 Marta Cervera¹⁹ | Jordi Ribera¹ | Manuel Fernández-Delgado²⁰ | Rosa Ayala⁹ |
 Antonia Cladera²¹ | María Carmen Mateos²² | María Jesús Vidal²³ | Jesús Feliu²⁴ |
 Ana Torres²⁵ | Gemma Azaceta²⁶ | María José Calasanz²⁷ | Anna Bigas^{1,28,29} |
 Manel Esteller^{1,29} | Alberto Orfao^{29,30} | Josep Maria Ribera^{1,2}  | Eulalia Genescà¹ 

Graphical Abstract



Genetic evolution and relapse-associated mutations in adult T-cell acute lymphoblastic leukemia patients treated in PETHEMA trials

Celia González-Gil¹ | Thaysa Lopes^{1,^} | Mireia Morgades^{2,^} | Francisco Fuster-Tormo¹ | Pau Montesinos³  | Carlos Rodríguez Medina⁴ | Lourdes Hermosín⁵ | Teresa González-Martínez⁶ | María-Paz Queipo⁷ | José González-Campos⁸ | Pilar Martínez-Sánchez⁹ | Marina Díaz-Beya¹⁰ | Rosa Coll¹¹ | Clara Maluquer¹² | Lurdes Zamora^{1,2} | Teresa Artola¹³ | Ferran Vall-Llovera¹⁴ | Mar Tormo¹⁵ | Anna Torrent²  | Carolina Martínez-Laperche¹⁶ | Cristina Gil-Cortés¹⁷ | Pere Barba¹⁸ | Marta Cervera¹⁹ | Jordi Ribera¹ | Manuel Fernández-Delgado²⁰ | Rosa Ayala⁹ | Antonia Cladera²¹ | María Carmen Mateos²² | María Jesús Vidal²³ | Jesús Feliu²⁴ | Ana Torres²⁵ | Gemma Azaceta²⁶ | María José Calasanz²⁷ | Anna Bigas^{1,28,29} | Manel Esteller^{1,29} | Alberto Orfao^{29,30} | Josep Maria Ribera^{1,2}  | Eulalia Genescà¹ 

Correspondence: Eulalia Genescà (egenesca@carrerasresearch.orgs)

Abstract

Relapse is the main cause of treatment failure in T-cell acute lymphoblastic leukemia (T-ALL). Despite this, data from adult T-ALL patients treated with specific chemotherapeutic regimens that examine predictive markers and describe relapse mechanisms are scarce. In this study, we studied 74 paired diagnosis-relapse samples from 37 patients homogeneously treated with three consecutive measurable residual disease-oriented trials to identify genetic determinants involved in relapse in adult T-ALL. Analysis of single-nucleotide variants and copy number alterations consistently found *N/KRAS* mutations (20% relapsed cases) at diagnosis and at relapse (resistance profile). *N/KRAS*^{mut} patients frequently relapse early during consolidation treatment. Relapse-specific mutations in *NT5C2*, *NR3C1*, *SMARCA4*, and *TP53* (40% relapse cases) were not detected at diagnosis by conventional molecular techniques (relapse profile). However, single-cell-based analysis revealed a very minor clone containing the *NT5C2*(p.R367Q) variant at diagnosis. Patients with the *NT5C2*(p.R367Q) variant mostly relapse later during maintenance treatment. Tracking the *NT5C2* variant by digital PCR confirm the expansion of the *NT5C2* clone at maintenance treatment. Overall, our exploratory analysis suggests a role for these genetic events, most of which have already been described in pediatric cases, driving resistance associated to specific chemotherapeutic agents, contributing to the relapse of a high proportion of adult T-ALL patients (60%).

¹Institut d'Investigació contra la Leucèmia Josep Carreras (IJC), Campus ICO-Germans Trias i Pujol, Universitat Autònoma de Barcelona, Badalona, Spain

²Servei Hematologia Clínica, ICO-Hospital Germans Trias i Pujol, Universitat Autònoma de Barcelona, Badalona, Spain

³Hospital Universitari i Politècnic La Fe, Valencia, Spain

⁴Hospital Universitario de Gran Canarias Dr. Negrín, Las Palmas de Gran Canarias, Spain

⁵Servicio Hematología Clínica, Hospital de Jerez, Jerez de la Frontera, Spain

⁶Servicio Hematología Clínica, Hospital Universitario de Salamanca, Salamanca, Spain

This is an open access article under the terms of the [Creative Commons Attribution-NonCommercial-NoDerivs](https://creativecommons.org/licenses/by-nc-nd/4.0/) License, which permits use and distribution in any medium, provided the original work is properly cited, the use is non-commercial and no modifications or adaptations are made.

© 2025 The Author(s). *HemaSphere* published by John Wiley & Sons Ltd on behalf of European Hematology Association.

INTRODUCTION

Treatment failure and relapse are the main causes of poor outcome in patients with T-cell acute lymphoblastic leukemia (T-ALL). Currently, 30%–50% of adult T-ALL patients treated with pediatric-inspired measurable residual disease (MRD)-oriented protocols suffer disease relapse.^{1–3} Alternative therapeutic approaches after progression are very limited. Recently, interest has been growing in identifying new prognostic and predictive markers of relapse, apart from MRD, with particular focus on evaluating the predictive value of genetic alterations identified in T-ALL. In this regard, the French cooperative group demonstrated the utility of a high-risk (HR) genetic signature defined by the absence of mutations in the *NOTCH1/FBXW7* signaling pathway and/or the presence of *PTEN* alterations and/or *RAS* mutations to identify adult⁴ and childhood⁵ T-ALL patients with high probability of relapse, irrespective of their MRD status.

In recent years, multi-omics techniques, including single-cell (SC)-based approaches, have become feasible for more detailed investigation of unique genetic profiles and markers involved in relapse in T-ALL patients through the analysis of triplets of DNA samples at diagnosis (DX), remission, and relapse (RE). Such an approach has helped us understand relapse mechanisms and identify potential targets for new therapies.^{6–10} Collectively, these studies have highlighted the role of relapse-associated mutations in the *NR3C1*, *TP53*, *NT5C2*, and *CREBBP* genes, all of which are implicated in chemotherapy resistance in ALL. Most of the data arising from these studies corresponded to the pediatric BCP-ALL subtype. A few studies have also attempted to explore relapse-specific mechanisms in pediatric T-ALL¹⁰; *NT5C2* emerged from these as the most frequent gene-bearing relapse-associated mutations, although it had no prognostic implications.¹⁰ In another series of 19 triplets (DX remission/germline RE) of adult T-ALL analyzed by whole-genome sequencing (WGS), mutations in *SMARCA4* were exclusively detected in two relapse samples, suggesting a potential role for this gene in relapse.¹¹

Identifying gene mutations present exclusively at relapse, but absent from diagnostic samples, calls their origin into question. Conversely, the treatment patients receive could induce the emergence of these new alterations; in turn, treatment could act solely as a filter contributing to the selection and expansion of a very minor relapse clone that is already present at diagnosis. Computational modeling to estimate the exact divergence time between the primary and relapse clonal populations has been used to address this.^{9,11} In one study, most relapses occurred less than a year after diagnosis, suggesting the pre-existence of the relapse

population before the treatment began.¹¹ In contrast, results of other studies based on a tumor cell (proliferation) doubling-time model were consistent with the hypothesis that treatment can generate resistant mutations.⁹ Limitations of the models used in these predictions, the limited sensitivity of the molecular techniques used to detect these mutations at diagnosis, and the type of sample analyzed may at least partially explain their contradictory results regarding this unresolved puzzle.

In this study, we analyzed 74 paired DX–RE samples from 37 adult T-ALL patients, most of them homogeneously treated with two consecutive MRD-oriented trials in the Spanish Programa Español de Tratamientos en Hematología (PETHEMA) group, with the aim of identifying genetic determinants of relapse.

METHODS

Patient samples and treatment protocols

Seventy-four paired DX–RE samples from 37 adult T-ALL patients who had given their informed consent were obtained from the Spanish National DNA Bank Carlos III (PT13/0001/0037 and PT13/0010/0067), La Fe Biobank (PT13/0010/0026), the IGTP Biobank (PT17/0015/0045), and our research group collection (C.0003303). DNA was most commonly isolated from whole bone marrow (BM) and occasionally from peripheral blood (PB), including FACS-purified (side scatter [SSC]^{lo/int} of light in CD7⁺ CD45^{lo}) leukemia cells in samples with <70% blasts (FACS ARIA, Becton/Dickinson Biosciences, San Jose, CA), in cases with sufficient available cells. T-ALL was diagnosed according to the WHO2017/2022 criteria.¹² Patients were treated with MRD-oriented HR adult ALL protocols (LAL-AR/2003 [NCT00853008]¹³ and LAL-AR/2011 [NCT01540812]²), two trials for elderly patients (LAL-07OLD [NCT01366898]¹⁴ and LAL-07FRAIL [NCT01358201]¹⁵), and the ongoing clinical trial (LAL-2019 [NCT04179929]) (Table S1 and S2). Samples and clinical data were stored following standard operating procedures, in accordance with the Declaration of Helsinki. The study was approved by the Institutional Review Board of the Hospital Germans Trias i Pujol.

Identification of single-nucleotide variants (SNVs)

Targeted deep sequencing (TDS) to identify SNVs and indels was performed in 35 DX samples and 25 RE samples, as described elsewhere.¹⁶ The median coverage was 440X for diagnosis samples and

⁷Servicio Hematología Clínica, Hospital Virgen de la Victoria, Málaga, Spain

⁸Servicio Hematología Clínica, Hospital Virgen del Rocío, Sevilla, Spain

⁹Servicio Hematología Clínica, Hospital 12 de Octubre, Madrid, Spain

¹⁰Servicio Hematología Clínica, Hospital Clínic de Barcelona, Barcelona, Spain

¹¹Servei Hematologia Clínica, ICO-Hospital Josep Trueta, Girona, Spain

¹²Servei Hematologia Clínica, ICO-Hospital Duran i Reynals, Hospitalet del Llobregat, Barcelona, Spain

¹³Servicio Hematología Clínica, Hospital Universitario de Donostia, Donostia, Spain

¹⁴Servei d'Hematologia Clínica, Hospital Mútua de Terrassa, Terrassa, Spain

¹⁵Hospital Clínico Universitario de Valencia, Instituto de Investigación INCLIVA, Valencia, Spain

¹⁶Servicio Hematología Clínica, Hospital Gregorio Marañón, Madrid, Spain

¹⁷Servicio Hematología Clínica, Hospital General de Alicante, Alicante, Spain

¹⁸Servei Hematologia Clínica, Hospital Universitari de la Vall d'Hebron, Barcelona, Spain

¹⁹Servei d'Hematologia Clínica, ICO-Hospital Joan XXIII, Tarragona, Spain

²⁰Servicio Hematología Clínica, Hospital General Universitario de Castellón, Castellón de la Plana, Spain

²¹Servei Hematologia Clínica, Hospital Son LLàtzer, Palma de Mallorca, Spain

²²Servicio Hematología Clínica, Complejo Hospitalario de Navarra, Pamplona, Spain

²³Servicio Hematología Clínica, Complejo Hospitalario de León, León, Spain

²⁴Servicio Hematología Clínica, Complejo Hospitalario de San Millán y San Pedro, Logroño, Spain

²⁵Servicio Hematología Clínica, Hospital General de Segovia, Segovia, Spain

²⁶Servei Hematologia Clínica, Hospital Clínico Universitario Lozano Blesa, Zaragoza, Spain

²⁷CIMA LAB Diagnostics, Clínica Universidad de Navarra, Pamplona, Spain

²⁸Programa d'Investigació del Cancer, Institut Hospital del Mar d'Investigacions Mèdiques, Barcelona, Spain

²⁹CIBERONC, Barcelona, Spain

³⁰Departamento de Medicina, Centro de Investigación del Cáncer (IBMCC-CSIC/USAL), Instituto Biosanitario de Salamanca, CIBERONC, Universidad de Salamanca, Salamanca, Spain

Present address: Francisco Fuster-Tormo, Technology & Development Team, Veritas Intercontinental, Barcelona, Spain.

^These authors contributed equally to this work.

591X for relapse samples (Table S3). Briefly, a custom NGS panel (SureSelectXT HS Target Enrichment System for Illumina Multiplexed Sequencing Platforms, Agilent Technologies, Santa Clara, CA) was used to prepare libraries that were sequenced in an MiSeq instrument (Illumina, San Diego, CA). WGS was performed in 19 paired DX-RE samples, the median coverage being 95X. To increase the coverage obtained by the WGS analysis and reduce the possibility of missing subclonal SNV/indels, we assessed 14 DX and 4 RE samples by TDS in addition to WGS. We did not detect additional variants in any of the analyzed cases (data not shown). Mutations were retrieved through local gold standard pipeline analysis. Selected variants were classified as pathogenic, of uncertain significance, or benign when the majority (i.e., $\geq 6/10$) of the analyzed in silico predictors identified the variant as being in one of the three categories. Benign variants were excluded from further analyses.

Identification of copy number variants (CNVs)

CNVs were obtained using SNP arrays (CytoScan HD, Thermo Fisher Scientific, Waltham, MA) in 28 cases (56 paired DX-RE samples). Results were analyzed using the Chromosome Analysis Suite (ChAS v 4.0.0.385). Variants larger than 1 kbp, and covered by more than eight probes, were selected. Constitutional CNVs (i.e., SNPs) were excluded by filtering data using the Database of Genomic Variants (DGV), from Uddin et al.¹⁷ and Thermo Fisher's data on healthy controls (DNA from 2700 anonymous individuals across the globe). The FACETS tool¹⁸ was applied to retrieve CNV data from WGS for six additional cases (12 paired samples). CNV analyses were not done for three cases (six paired DX-RE samples). In total, CNV data were available for 34/37 cases. Variant allele frequency (VAF) and cancer cell fraction (CCF) estimation from CNV data are detailed in the Supporting Information.

Digital PCR (dPCR) experiments

The QuantStudio™ 3D Digital PCR system (Thermo Fisher Scientific) with a custom probe to quantify the number of DNA molecules with the NT5C2(p.R367Q) variant (Thermo Fisher Scientific) was used. We assessed the presence of the NT5C2(p.R367Q) variant in 300 ng of DNA/sample from three patients. In total, 13 samples obtained at diagnosis and at different times during follow-up were available (Table 4). To assess the limit of blank (LOB), we ran eight chips with 300 ng of non-mutated DNA. A minimum of six positive points was stipulated. To assess the limit of detection (LOD), we prepared serial dilutions with the relapse sample, mixed with non-mutated DNA. The dPCR assay achieved a sensitivity of $<0.01\%$ (10^{-4}). Results of the dPCR were expressed as the percentage of DNA copies with the mutation/total DNA copies analyzed.

SC DNA sequencing and analysis

Paired DX-RE samples from three adult T-ALL patients (PAT36, PAT30, and PAT24) were analyzed. The diagnostic sample from PAT24 was mixed with 8% non-leukemic cells (mononuclear cells from a healthy donor) to have enough normal cells to normalize the copy number data. The diagnostic sample of this patient was encapsulated three times to gain sensitivity (Table S5). In that particular case, sensitivity was 5×10^{-4} (above the technique's LOD; Supporting Information). In total, eight samples were analyzed by SC (five DX and three RE samples).

A custom single-cell DNA sequencing (scDNA-seq) panel including 156 amplicons covering genes with somatic mutations and

CNVs, previously detected by TDS and SNP arrays, was designed. Amplicons covering areas flanking those regions carrying CNV were also included to normalize the copy number data (Table S6). ScDNA-seq was performed using the Tapestry® Platform V2 (Mission Bio, San Francisco, CA) according to the manufacturer's instructions (PN_3354H1). DNA libraries were sequenced on a NovaSeq 6000 instrument (Illumina) using a 150-bp paired end-run strategy. Sequencing and sample quality metrics are indicated in Table S5. FASTQ files generated by the NovaSeq instrument were processed using the cloud-based Tapestry Pipeline (Tapestry DNA v.2). With this pipeline, adaptor-sequence trimming, read alignment, and variant calling were done for all the samples except for the diagnostic samples of PAT24, which were analyzed using the Merge Runs option (v1.0 Tapestry Pipeline). In all cases, the reads were mapped to the GRCh37/hg19 human reference genome using the BWA-MEM aligner. Sequences matching the targeted genomic regions were kept and the remaining barcodes removed. GATK 3.7 was used for cell genotyping and variant calling. The PAT36 and PAT30 loom files generated by the Tapestry pipeline were loaded into the Tapestry Insight v2.2 software for pre-filtering and exploratory analysis. In the case of PAT24, h5 files were analyzed with the Mosaic program (v3.0.1) using a modified multi-sample DNA-only notebook (MissionBio). The workflow for variant and clonal marker identification with Mosaic was the same as that used with Tapestry Insight. More details are provided in the Supporting Information.

Statistical methods

Differences between groups for continuous variables were assessed by Wilcoxon rank-sum (paired variables) and Mann-Whitney tests (unpaired variables). For categorical variables, Fisher's exact test was used. Values of $p < 0.05$ were considered to indicate statistical significance; values of $p < 0.1$ were taken to suggest a non-significant trend. All statistical analyses were carried out with GraphPad (v10) and R (v4.3.2). Figures were generated in R (v4.3.2) using the TimeScape package (v1.26.0), GraphPad (v10) and BioRender.

RESULTS

Heterogeneous origin of relapse leukemia cell clones

To retrieve genomic information from paired DX-RE DNA samples, we analyzed SNVs and indels in 37 adult T-ALL patients and CNVs in 34 of these same cases (Table S7). First, we focused on the distribution and presence/absence of variants at DX versus RE. The medians [range] of SNV/indel alterations at DX and RE were 3 [1–9] and 4 [0–16], respectively ($p = 0.27$); and the medians of CNV alterations at DX and RE were 3 [0–15] and 4 [1–16], respectively ($p = 0.28$) (Figure 1A). In contrast, a statistically significantly higher CCF in SNVs/indels was observed when we compared common variants between DX and RE whose CCF varied. The median CCF for SNVs/indels was 81.3 [5.6–110.7] at DX and 84.8 [11.6–134.4] at RE ($p = 0.036$). For CNVs, the median CCF was 100 [10–113] and 100 [19–123] at RE ($p = 0.07$). The results suggested a slight selection of under-represented SNV/indels at DX in the RE samples (Figure 1B). Differences between DX and RE samples were also observed in the distributions of the variants. Thus, for SNVs/indels, around half (48.3%) of the 205 variants identified were shared by the DX and RE samples, one-third (32.2%) were restricted to RE, and the other 19.5% were only present at DX. Of the 199 CNVs identified, 66.8% were shared by DX and RE, 22% were only present at RE, and 11% were restricted to the DX samples. Based on the percentage of each

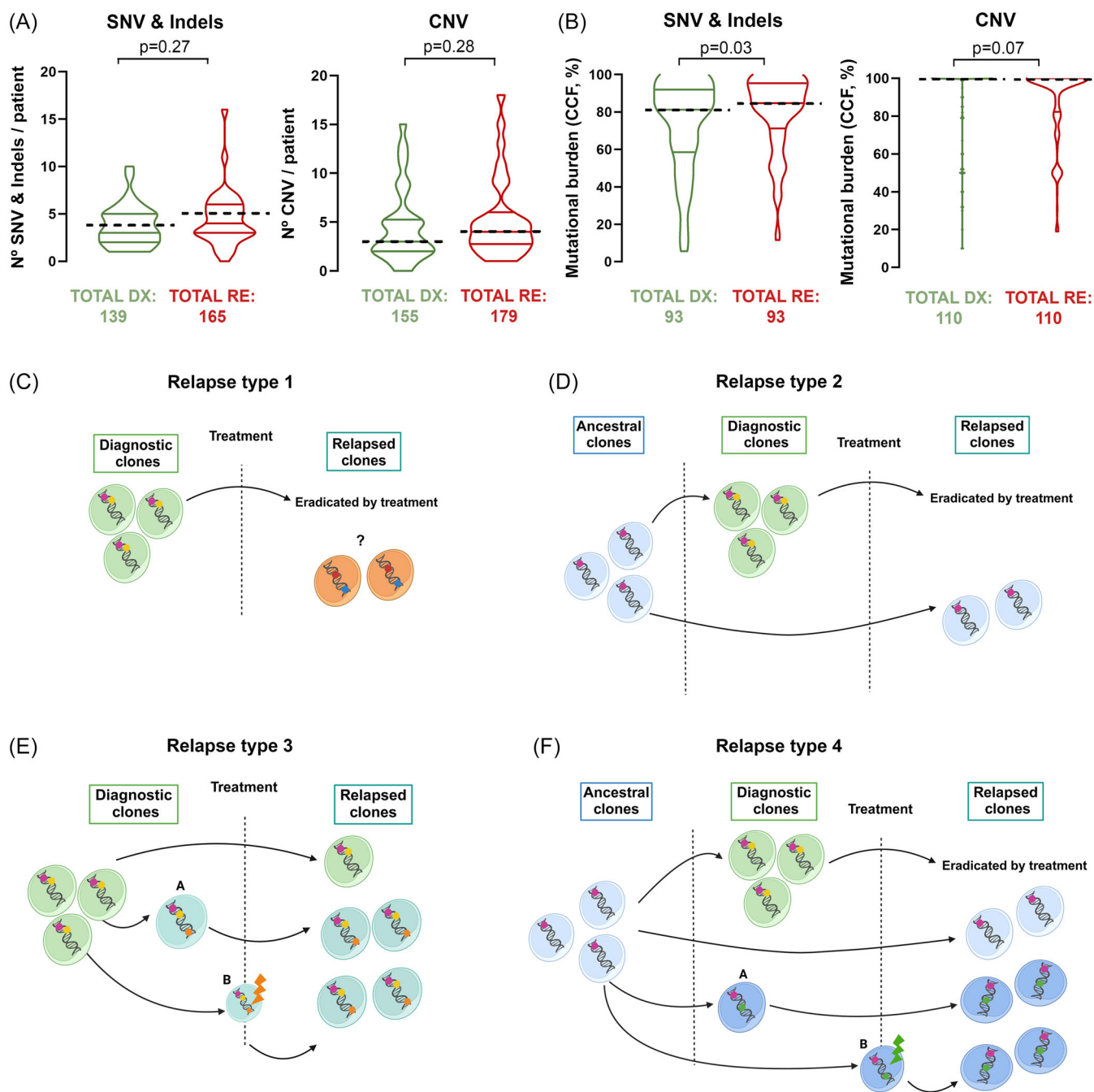


FIGURE 1 Variant distribution and clonal evolution models in bulk leukemia. (A) Differences in the number of variants per patient between diagnosis and relapse (Mann-Whitney U test). Differences in single-nucleotide variants (SNVs) and indels, and in copy number variants (CNVs) are shown on the left and right, respectively. (B) Differences in the mutational burden quantified by the cancer cell fraction (CCF), considering only common variants whose CCF differs between DX and RE (Wilcoxon test). Differences in SNVs and indels and in CNVs are shown on the left and right, respectively. (A, B) The median CCF is indicated by the dashed line. The number of variants assessed are indicated below each graph. Clonal evolution models in bulk leukemia: (C) Relapse leukemia has an origin independent of diagnosis. The diagnosis clone is represented in green with its specific variants shown in yellow and pink; the relapse clone is represented in orange with its specific variants shown in red and blue. (D) Relapse leukemia evolves from an ancestral clone. The diagnosis clone is represented in green with specific variants shown in yellow and pink; the relapse clone evolves from an ancestral clone, with fewer variants than the main diagnosis clone. (E) The relapse clone evolves from the main diagnosis clone by acquiring a new variant at diagnosis (A) or during treatment (B). The most common diagnosis clone is represented in green with common diagnosis and relapse variants shown in yellow and pink; the relapse clone is represented in turquoise with the specific relapse variants shown in orange. (F) The relapse clone evolves from an ancestral clone through the acquisition of new variants at diagnosis (A) or during treatment (B). The diagnosis clone is represented in green with a diagnosis-specific variant shown in yellow; the ancestral clone is represented in light blue with an ancestral variant shown in pink; the relapse clone is represented in dark blue with the specific relapse variants shown in green.

alteration, our data suggest that CNV alterations are genetic events that are more frequently retained at T-ALL progression.

Further analysis of the distribution of these variants by patient revealed four relapse-associated patterns of decreasing frequencies: (i) patients with common DX-RE, some RE-specific and other DX-specific alterations ($n = 21$; 56.7%) (Figure S1A); (ii) relapse patients with shared variants at DX and RE, and others detected only at RE ($n = 12$, 32.4%) (Figure S1B); (iii) patients with common DX-RE variants and some restricted to DX ($n = 3$, 8.1%) (Figure S1C); and (iv) relapse patients with a leukemia with a completely different genetic profile ($n = 1$, 2.7%) (Figure S1D). Based on the same data, we were able to define a hypothetical patient's specific clonal progression model, which would identify a few patients whose relapsed leukemia arises from a genetically different clone from that observed at diagnosis (Figure 1C, RE type 1). For the other patients, relapse clones evolve from a less genetically variable pre-leukemic clone (Figure 1D, RE type 2), or from the main clone found at diagnosis (Figure 1E, RE type 3) or a pre-leukemic clone (Figure 1F, RE type 4). In the latter two cases, relapse-specific mutations would be acquired before or during treatment (paths A and B, respectively). At this point, our descriptive analysis becomes unable to clarify the origin of these relapse-specific mutations.

Identification of relapse-associated genetic profiles in adult T-ALL patients

To search for genetic alterations that could drive relapse in adult T-ALL, we evaluated the distribution of the variants of recurrently altered genes (in at least four patients) in our DX-RE T-ALL cohort, identified at diagnosis and relapse. For this purpose, we defined a gene/genetic alteration to drive resistance whenever more than 75% of its variants were present at DX and RE. Thus, *CDKN2A/B*, *FBXW7*, *RPL22*, *PHF6*, *RUNX1*, *del(6q)*, *DNMT3A*, and *N/KRAS* were genes with 100%, 76.9%, 80%, 100%, 100%, 100%, 100%, and 83.3% of their variants present at DX and RE, respectively. We grouped these genes together into what we named the "resistance profile." Likewise, if more than 75% of variants of a gene were only detected at relapse, we classified that gene as a relapse-associated gene/genetic alteration (Figure 2A, orange and red squares, respectively). That was the case of *SMARCA4* (100%), *NT5C2* (100%), *TP53* (100%), and *NR3C1* (85.71%) genes globally considered as the "relapse-associated profile." Finally, the genes with mutations in *NOTCH1*, *PTEN*, *BCL11B*, *CTCF*, *JAK3*, *JAK1*, *CDKN1B*, *CDK6*, and *ETV6* were not categorized into either of the two groups. Notably, they did not form a distinct group on their own.

To demonstrate that the two genetic profiles (resistance and relapse) had arisen by mutually exclusive events, we investigated the potential relationship between genes belonging to the two profiles (Figure 2B). We observed that, for the -resistance profile genes, only *N/KRAS* mutations were mutually exclusive with the alterations in those genes included in the relapse profile ($OR = 0$; $p = 0.01$). This suggests a role for *N/KRAS* gene mutations driving patient relapse. The observation that CNVs were not expanding at RE (same CCF median, Figure 1B), suggests a potentially more supportive role in leukemia development and maintenance, of the other alterations within the resistance profile (*CDKN2A/B*, *FBXW7*, *RPL22*, *PHF6*, *RUNX1*, *del(6q)*, and *DNMT3A*), rather than a driving relapse effect. This hypothesis could also help explain the co-occurrence of *NT5C2* gene mutations and *del(6q)* ($OR = 14$; $p = 0.06$) (Figure 2B).

To support our hypothesis about the role of the two gene profiles in disease relapse, we investigated the potential association between the two genetic profiles and time to relapse. The median time from

complete remission (CR)-RE was 4.5 [1.3–21.8] months for patients with a resistance genetic profile (*N/KRAS* mutated patients) and 9.5 [4.9–19.77] months for those with the relapse profile (patients with alterations in *TP53*, *NT5C2*, *SMARCA4*, and *NR3C1*) ($p = 0.022$). This result supports the hypothesis that two different relapse mechanisms arise from distinct genetic lesions and is consistent with our previous genetic findings. Considering all the data, our analysis suggests a role of genetic alterations as drivers of relapse in 60% of the patients in our cohort. Most frequently (40% of cases) these alterations correspond to point mutations in *NT5C2*, *SMARCA4*, and *NR3C1*, along with *TP53* deletions, that were undetected at diagnosis. The presence of *N/KRAS* mutations could be responsible for a further 20% of relapse cases (Figure 2C). Since *N/KRAS* gene mutations were already evident by the time of DX, *N/KRAS* was considered a potential genetic marker predicting relapse. We previously demonstrated the role of these mutations in identifying patients with a high probability of relapse in a large series of adult samples studied at diagnosis.¹⁶

Tracking *NT5C2* relapse-specific genetic variants

The mechanism by which relapse-specific genetic alterations (which, by definition, go undetected at diagnosis by TDS analysis, and emerge at relapse) arise, as well as the exact moment they might occur, are not fully understood. To address these gaps in our knowledge, we focused on *NT5C2* mutations. We tracked the *NT5C2*(p.R367Q) variant by the highly sensitive (10^{-4} , i.e., two orders of magnitude more sensitive than TDS) dPCR method in 13 serial samples obtained at DX and during follow-up until the relapse of the patients (Table S4). Our results revealed detectable levels of the *NT5C2*(p.R367Q) variant after induction treatment in PAT24, and a positive result below the technique's LOD for PAT24 and PAT14 at DX (Figure 3A,B). Digital PCR was, again, not sensitive enough to clearly detect the *NT5C2*(p.R367Q) point mutation (an insufficient amount of the DX sample from PAT16 precluded the possibility of detecting the mutation by dPCR).

Next, dPCR-based serial analysis of patient samples revealed a consistent subsequent increase in the number of *NT5C2*(p.R367Q) variant copies from late consolidation to maintenance therapy, suggesting that, in all three cases, the treatment applied during maintenance allowed the expansion of the *NT5C2*(p.R367Q)-positive leukemic clone (Figure 3A–C). This is consistent with the relapse of patients with the *NT5C2* mutation being associated with the maintenance block ($p = 0.01$) (Table 1). Similarly, there was a non-significant trend toward the relapse of patients, with *N/KRAS* mutations being associated with the consolidation treatment ($p = 0.06$).

Finally, we compared the sensitivity of next-generation flow cytometry (NGFC) with that of dPCR to track *NT5C2*-mutated clones. Our results showed the latter technique to be more sensitive for monitoring the *NT5C2*(p.R367Q) clone after consolidation treatment, suggesting the potential value of using dPCR to monitor resistant clones in clinical trial settings.

SC analysis confirms the *NT5C2* variant is already present at diagnosis

To confirm the different patterns of clonal evolution inferred from bulk mutational analysis, and to demonstrate the presence of relapse-specific variants at diagnosis, we performed SC of three paired DX-RE patient samples. We analyzed 57,782 cells for a total of eight samples that presented relapse-associated variants in *NR3C1*, *SMARCA4*, *NT5C2*, and/or *TP53* genes. A median of 6968 [5834–8758] cells per

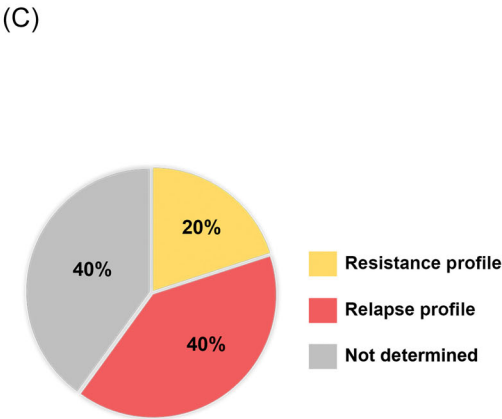
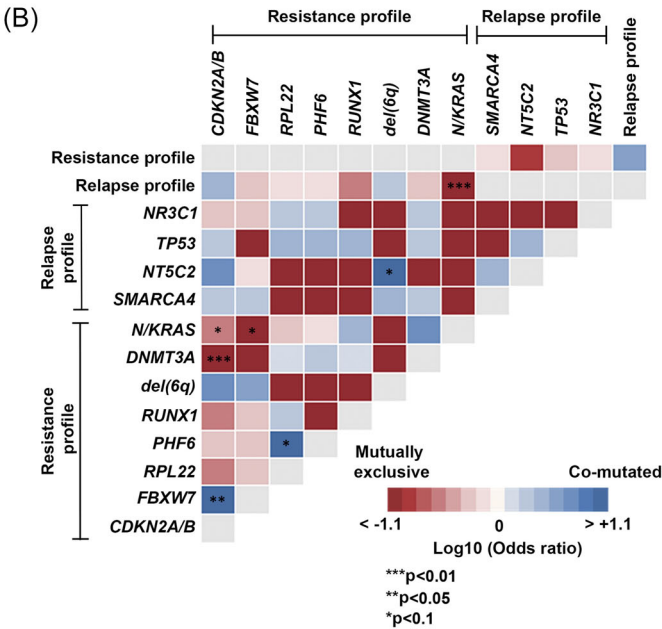
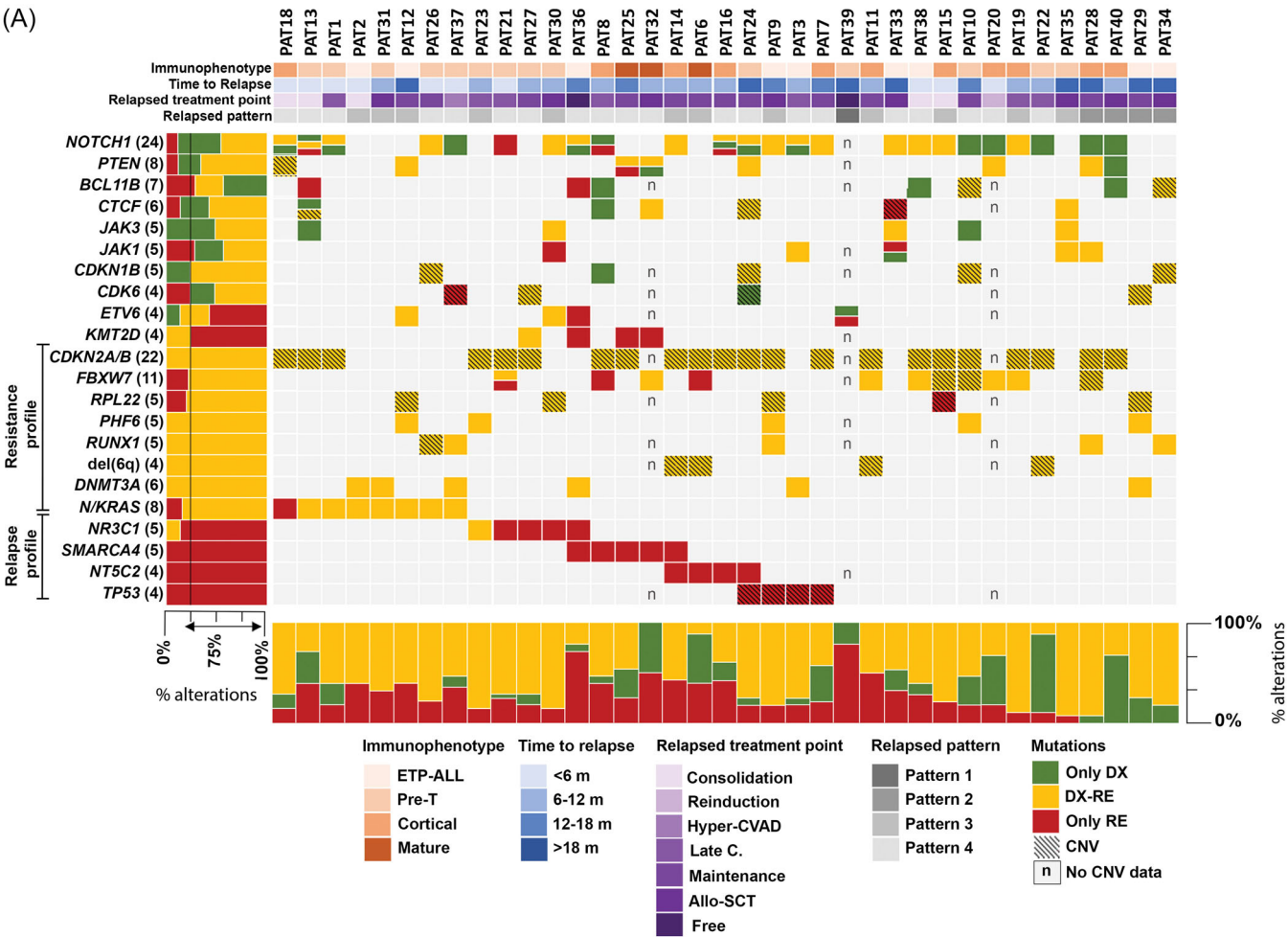


FIGURE 2 (See caption on next page).

FIGURE 2 Genetic profiles associated with relapse in adult T-ALL. (A) Genetic landscape of the paired samples. Only genes mutated in at least four patients are shown. Diagnosis-specific variants are shown in green, relapse-specific variants are shown in red, and common variants at diagnosis and relapse are shown in orange. Relapse characteristics for each patient are indicated above each figure. The frequency of each type of variant per gene (diagnosis-specific, relapse-specific, or common diagnosis-relapse) is shown on the right. Gene/genetic alteration with more than 75% of its variants detected at DX and RE are assigned to resistance profile group, and those with more than 75% of its variants only detected at RE are classified as having a relapse profile. The frequency of each type of variant per patient is shown at the bottom. (B) Pairs of associations of the frequent mutated genes and the defined relapse profiles. Positive associations (\log_{10} odds ratio >0) are represented in blue; negative associations (\log_{10} odds ratios <0) are shown in red. (C) Cohort classification according to the defined relapse profiles. Patients with the resistance profile are shown in yellow; those with the relapse-specific profile are identified in red; and unclassified patients are shown in gray.

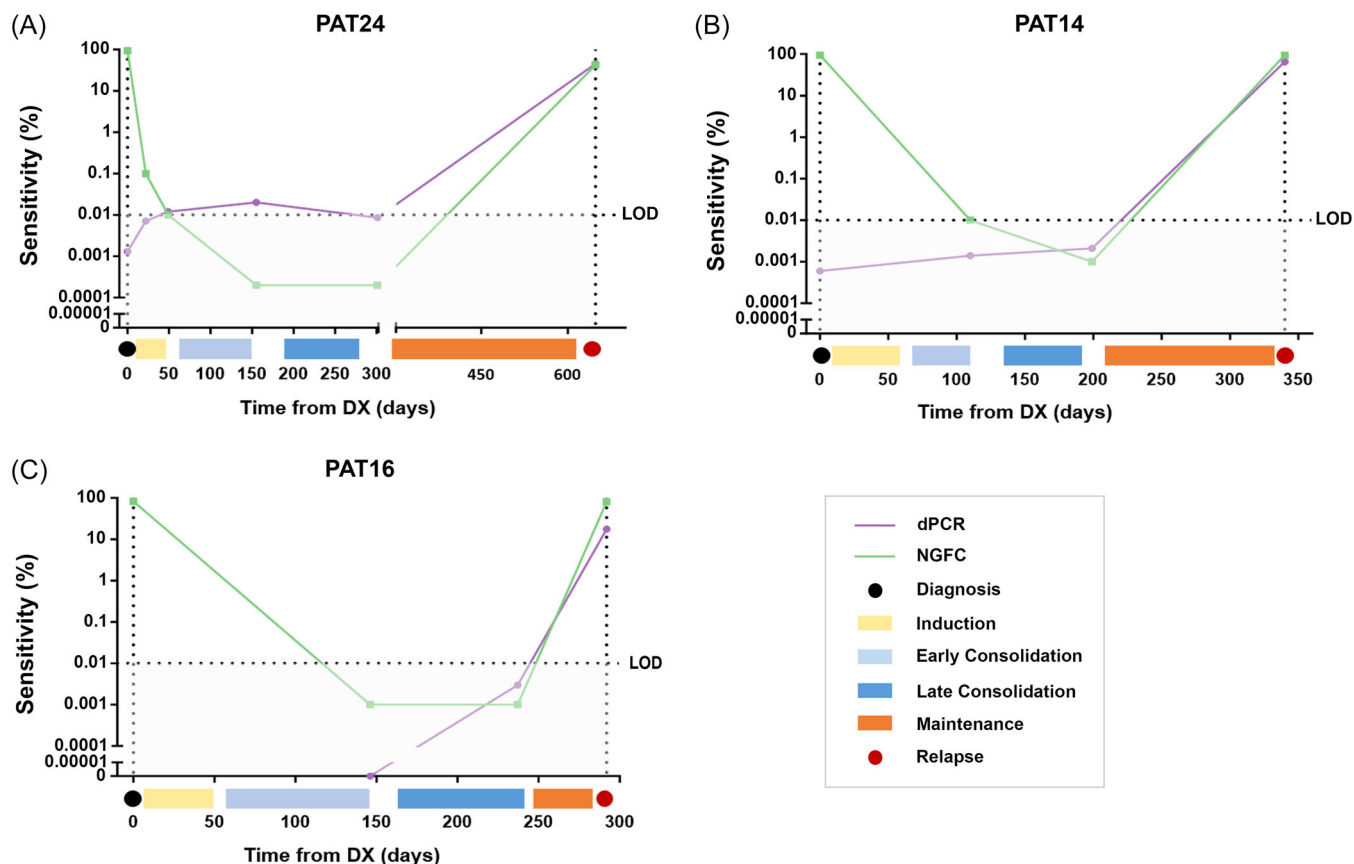


FIGURE 3 dPCR-based identification of the NT5C2(p.R367Q) mutation versus NGFC-MRD levels in T-ALL samples obtained at early treatment times. (A–C) The sensitivity of the dPCR (Y-axis) considers the number of DNA copies with the mutation relative to the total number of DNA copies (purple line). Measurable residual disease (MRD), quantified by the next-generation flow cytometry (NGFC), is represented by a green line. The limit of detection (LOD) is indicated with a horizontal dashed line. The days elapsed between diagnosis and relapse are shown on the X-axis. The different treatment blocks are represented by different colors.

sample and 85 [64.5–109.5] reads per amplicon per cell (Table S5) were obtained. Comparing the mutational profiles obtained in bulk DNA and SC DNA sequencing revealed the presence of the NR3C1(p.R569W) variant at a low VAF (0.9%) in the SC analysis. This was not present in the bulk analysis, and so highlights the greater sensitivity of the SC approach compared with that obtained under our bulk sequencing conditions (Table S8).

Next, we investigated the co-occurrence and defined the potential order of acquisition of all filtered mutations in the SC experiments by focusing on the clonal origin of the relapse-associated mutations in *SMARCA4*, *NR3C1*, and *NT5C2* genes. We detected three positive cells for *SMARCA4*(p.R425Q) and *NR3C1*(p.A578T) at DX in PAT36 (Table S8), fewer than the five needed to conclude the existence of an independent clone from the SC analyses (Figure 4A). The clonal architecture of PAT36 highlighted the role of *TET2*(p.K1001fs) mutations in

initiating leukemia. Expansion of the main leukemic clone occurred with the acquisition of a double hit on the *TET2* gene (*TET2*[p.K1001fs] + *TET2*^{del}) after the acquisition of the *DNMT3A*(p.R882H) variant in heterozygosity; both genes affect the methylation pattern in the leukemic cell.¹⁹ Of note, PAT36 was of advanced age at diagnosis. The clone containing these alterations was also the main clone identified at RE in 33% of leukemic cells, together with a second clone containing the *SMARCA4*(p.R425Q) variant in homozygosity (27% leukemic cells at RE). The main RE clone evolved from the *TET2*(p.K1001fs) + *DNMT3A*(p.R882H) + *TET2*^{del} clone identified at DX and acquired the *NR3C1*(p.A578T) and *KMT2D*(p.R1299H) variants (Figure 4A and Table S9), among other variants. Likewise, in PAT30, SC analysis revealed three leukemic cells positive for *NR3C1*(p.G290E), which also did not constitute a DX clone. In this case, T-ALL leukemia originated from a *KMT2A*(p.R2940P) + *ETV6*(p.T86fs) + *KDM5A*^{del} clone. The clone

TABLE 1 Relationship between treatment times and relapse-associated gene profiles in the bulk sample.

Genes	NR3C1			SMARCA4			NT5C2			TP53		
	N/KRAS n = 29	Non-mutated n = 8	Mutated n = 8	p	Non-mutated n = 32	Mutated n = 5	p	Non-mutated n = 33	Mutated n = 4	p	Non-mutated n = 30	Mutated n = 4
Treatment												
Early consolidation (n = 5)	2 (6.9)	3 (37.5)	0 (0)	0.06	5 (15.6)	0 (0)	>0.99	4 (12.1)	0 (0)	>0.99	5 (13.3)	0 (0)
Reinduction (n = 1)	1 (3.8)	0 (0)	0 (0)	>0.99	1 (3.1)	0 (0)	>0.99	1 (3)	0 (0)	>0.99	1 (3.6)	0 (0)
Hyper-CVAD (n = 1)	0 (0)	1 (12.5)	0 (0)	0.2	1 (3.1)	0 (0)	>0.99	1 (3)	0 (0)	>0.99	1 (3.3)	0 (0)
Late consolidation (n = 7)	6 (20.7)	1 (12.5)	2 (25)	>0.99	5 (15.6)	2 (40)	0.23	7 (21.2)	0 (0)	0.6	6 (20)	1 (25)
Maintenance (n = 13)	11 (37.9)	2 (25)	1 (12.5)	0.69	11 (34.4)	1 (20)	>0.99	9 (27.2)	4 (100)	0.01	11 (36.6)	2 (50)
Allo-SCT (n = 8)	7 (24.1)	1 (12.5)	0 (0)	0.66	7 (21.9)	1 (20)	>0.99	8 (24.2)	0 (0)	0.56	6 (20)	1 (25)
Free of treatment (n = 2)	2 (6.9)	0 (0)	0 (0)	>0.99	1 (3.1)	1 (20)	0.26	2 (6)	0 (0)	>0.99	1 (3.3)	0 (0)

Note: Results are expressed as number of cases (percentage).

expands with the acquisition of JAK3(p.M511I) + NOTCH1(p.V1676D) variants. This was the major clone at DX (74%). The clone acquired the JAK1(p.Y652H) mutation and after, probably, NR3C1(p.G290E). However, the SC analysis was not able to detect the NR3C1(p.G290E)-containing clone at DX, due to the technique's limited sensitivity. The major clone at RE (78.8% leukemic cells) contained the NR3C1(p.G290E) variant (Figure 4B and Table S9). In PAT24, with a NT5C2 in the relapse detected by TDS, three replicates of the DX sample were analyzed in parallel, sequencing a total of 21,553 cells. Of these, 11 were positive for the NT5C2(p.R367Q) variant (Table S8). SC analysis identified a clone consisting of five leukemic cells positive for this mutation at DX (Figure 4C and Table S9). Here, the leukemia was initiated by the acquisition of several MYB mutations (pD13E and pE14delinsGK) and a MYB^{dup}, and other structural alterations (RB1^{del}, DNMT2^{del}; +19 and +21), being the major clone at DX. Next, the clone acquired the NT5C2(p.R367Q) variant, which was the last clone identified at DX. The main clone at RE (87.41% of leukemic cells) evolved from the NT5C2(p.R367Q) clone by acquiring the CCND3(p.E248fs) variant. TP53^{del} was present in almost 40% of the RE NT5C2(p.R367Q)-positive leukemic cells (Table S10), suggesting the partial co-existence of the two alterations in the leukemia cells, also at DX (Figure 4C).

DISCUSSION

In this study, we describe patterns, dynamics, and genetic markers associated with clonal evolution and relapse of adult T-ALL patients with the aim of anticipating such adverse events and helping delineate potential preventive therapeutic interventions. Comparing the mutational profiles of T-ALL patients at diagnosis and relapse, we suggested the presence of two genetically independent mutagenic profiles. We defined a resistance profile, characterized by the presence of N/KRAS mutations, which were present in the main clone at DX (VAF > 40%, representing >80% of T-ALL cells), and persisted throughout treatment, re-emerging as the main clone at relapse. This specific mutational profile in T-ALL is not common in BCP-ALL, where RAS mutations are frequently subclonal at diagnosis and expanded at relapse.²⁰⁻²² In fact, N/KRAS mutations have been specifically associated with patients with an immature ETP-ALL immunophenotype,^{16,23} in contrast to the more heterogeneous distribution in B-ALL.⁷ Patients with N/KRAS mutations are resistant to frontline chemotherapy drugs such as methotrexate and prednisone, which might help explain the persistence of clones containing these mutations during treatment and subsequent relapse.^{20,24,25} In our cohort, patients with N/KRAS mutations had a median RE time of 4.5 months, consistent with the positive correlation we found between relapse and consolidation treatment (usually consolidation treatment is administered 2–6 months after DX). Therefore, a different frontline therapeutic schedule for these patients might help achieve a better response and outcome. In that sense, it would be worthwhile exploring a frontline treatment approach based on the use of BH3 mimetics (e.g., venetoclax and navitoclax) in these group of patients, since anti-apoptotic drugs are known to be more effective in immature T-ALL leukemias.²⁶ Although mutations in N/KRAS genes are not the unique cause of the relapse of patients with the resistance profile, they can serve as genetic marker of relapse, as we and others have previously demonstrate.^{16,27}

In parallel, we identified a second mutational profile, which was found almost exclusively among the relapse samples, consistent with previous findings.^{6,9,20,28,29} Most of these genes have also been associated with chemotherapeutics used in T-ALL treatment. The NT5C2 gene codes for an enzyme that inactivates the monophosphates that mediate the cytotoxic effects of 6-mercaptopurine and 6-thioguanine,³⁰ two drugs used in the maintenance block in ALL

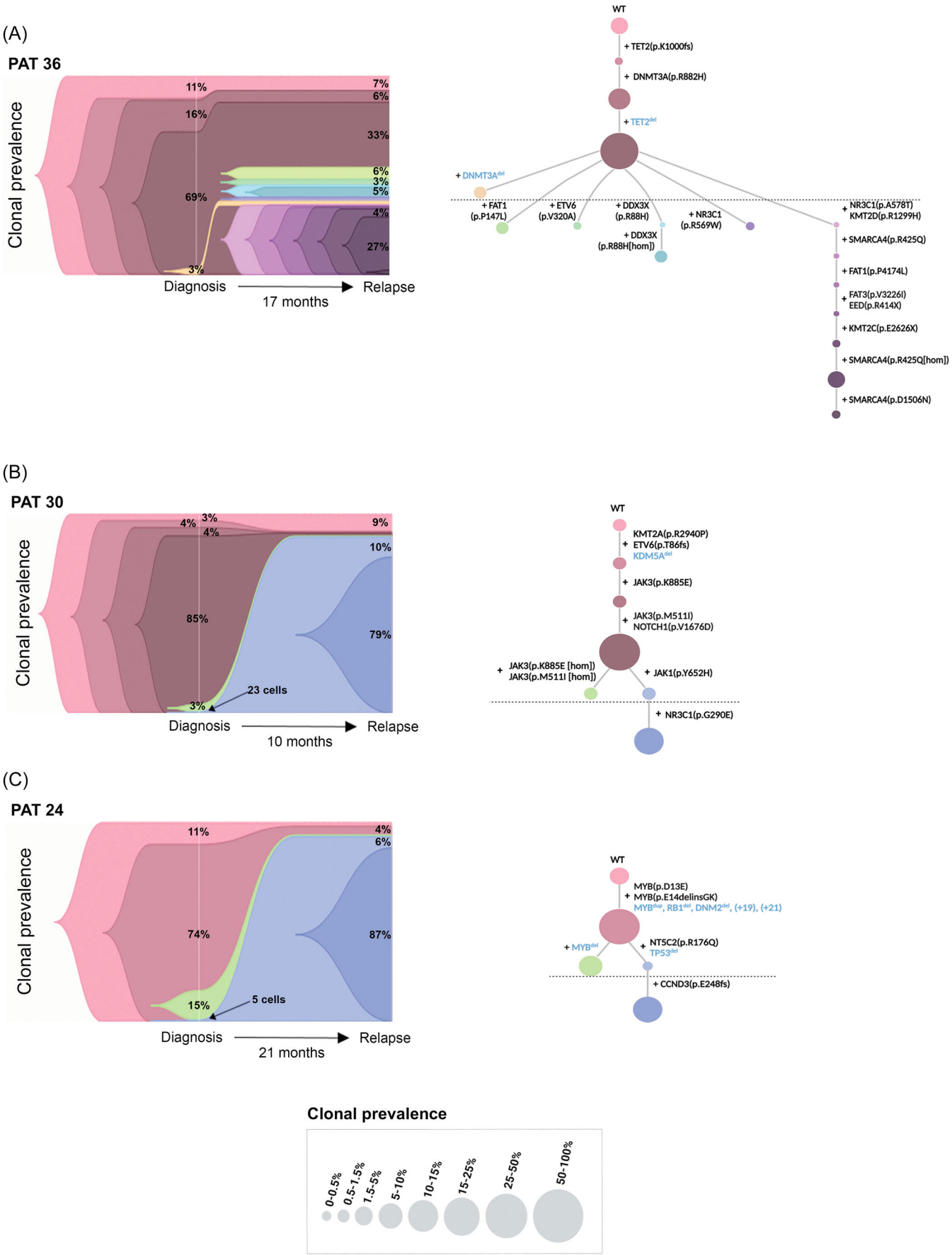


FIGURE 4 (See caption on next page).

FIGURE 4 Identification of the NT5C2(p.R367Q) variant at diagnosis by single-cell analysis. (A–C, Left) The fish plot shows the clonal evolution from diagnosis to relapse of three T-ALL patients carrying relapse-specific variants: (A) NR3C1(p.A578T) and SMARCA4(p.R425Q); (B) NR3C1(p.G290E); and (C) NT5C2(p.R176Q) and TP53^{del}. Each color represents a clone. The minimum clone size was five cells. The percentages show the proportion of cells that made up each clone at diagnosis (middle of fish plot) and relapse (right side of fish plot). Only percentages ≥3 are shown. (A–C, Right) Phylogenetic trees illustrating the maximum likelihood of the order in which mutations were acquired during T-ALL development in the indicated patients. The colors used to represent each clone are the same as those used in the fish plots (left). Mutational history was reconstructed from the genotype data from the samples obtained at diagnosis and relapse. The size of the circle denotes the relative clone size in the samples (integrating the information from diagnosis and relapse). The new variant acquired at each step is noted. The CNVs and SNVs are indicated in blue and black, respectively. The dashed line separates the last DX clone and the first RE clone.

patients, thereby conferring resistance to these drugs in cells carrying mutations of this gene.^{6,31–33} Similarly, mutations in NR3C1, a gene encoding a glucocorticoid receptor, prevent glucocorticoid transcriptional activation activity, generating resistance to prednisolone.⁹ TP53 alterations have been associated with worse response to treatment,³⁴ since cells with TP53 alterations are resistant to chemotherapy drugs that induce double-strand DNA breaks,³⁵ such as Ara-C, a drug used in T-ALL treatment. Conversely, SMARCA4 is a component of the SWI/SNF chromatin remodeling complex, and its function in T-ALL remains unknown. Although mutations in this gene have been associated with resistance to ibrutinib and venetoclax, in other hematological malignancies,³⁶ there is no evidence that they are involved in mechanisms of resistance to a specific chemotherapeutic agent used in the treatment of T-ALL patients. Their effect may therefore more likely be related to an epigenetic-driven relapse mechanism.

We focused on patients carrying the NT5C2(p.R367Q) mutation, which consistently showed disease relapse during maintenance treatment, linked to 6-mercaptopurine resistance, as previously discussed. It is important to mention that not all the patients in our cohort who received 6-mercaptopurine then experienced a relapse (Figure 2A), suggesting that chemotherapy might not cause this mutation to arise. Notably, SC studies showed the presence of the NT5C2(p.R367Q) mutation in a very small subset of leukemic cells at diagnosis. Together, these findings suggest that T-ALL patients who experience disease relapse may already possess all the genetic variability required for that at diagnosis. In a clinical setting, it will be interesting to implement a prospective screening for NT5C2 mutations in T-ALL patients allocated to the chemotherapy arm after consolidation and provide a different chemotherapeutic regimen, avoiding the use of 6-mercaptopurine, in the positive cases. This test will also help to validate the relationship of NT5C2 and maintenance therapy.

Despite our findings, we could not identify genetic markers that drive relapse in 40% of the patients in our cohort, with the techniques we employed. For these patients, there was a no clear selection pressure from the treatment and no selection of leukemia cell clones with specific mutations at relapse. The results suggest that these patients might follow another/others relapse pathway/s.

A relapse mechanism known as “clonal drift” has recently been described in B- and T-ALL pediatric patients, in which there were no substantial changes in the genetic profile and the clonal composition of leukemia cells, but significant changes in the transcriptional and epigenetic profile were identified in relapse clones.^{37,38} In that sense, patients in the unclassified group presented a median of time to relapse of 12 [3–53] months, longer than those patients included in the resistance or relapse profile. Similar studies, all done in pediatric T-ALL cohorts, have also suggested that patients carrying mutations associated with drug resistance relapse earlier than those without these mutations.^{9,39} Therefore, further transcriptomic and epigenomic profiling of the remaining 40% of adult T-ALL patients will be valuable to identify additional relapse mechanisms. Expanding our study cohort by including more paired DX–RE samples would not only help to address to classify the other genetic events detected in relapse samples (e.g., KMT2D, RUNX1 mutations, or FBXW7 alterations), which could not

only be addressed in this study but also determine whether the unclassified relapse group represents a distinct type of relapse. This aspect remains unclear due to the limited number of paired cases available for analysis and the heterogeneity of the results.

Finally, the most paired DX–RE samples analyzed shared at least one genetic alteration at diagnosis and relapse, although the relapse sample showed a different clonal composition from that of primary leukemia. These findings are consistent with the hypothesis that leukemia follows an evolutionary process from diagnosis, through treatment, until relapse, in which clones adapt to the new environment shaped by the treatment thanks to their unique mutational profile. Clones containing resistant mutations will survive treatment and finally expand. Patients with the relapse-associated and resistance-related profiles identified here (relapse types 2, 3, and 4 of the bulk model) fit with this model, which is also described in BCP-ALL and in pediatric T-ALL cases.^{7,40,41} Furthermore, our study employed SC analysis to define the potential sequential order of acquisition of the genetic events and identify the mutational profile of the founder clone, as well as those mutations potentially responsible for the expansion of the resistant clone observed at RE. Although the number of patients analyzed was small, the SC analysis of the three patients belonging to the same evolutionary bulk model showed different genetic origins and evolutionary profiles of relapse, highlighting the great heterogeneity of the leukemia evolution and adaptation to treatment in T-ALL. These differences may be correlated with the range of abnormal functions of these genes in leukemic cells (i.e., a direct drug-resistant effect and/or epigenetic mechanisms). Our data also suggest that identifying the genetic profile of the founder clone is a pre-requisite for eradicating leukemia.

In summary, we have described genetic profiles that help us account for 60% of the relapsed T-ALL cases in our cohort. Most of these genes have already been described in pediatric cases (e.g., NT5C2, N/KRAS, and TP53). However, the frequency of these events and the timing of clone expansion is different depending on the type of analyzed patient (adult or pediatric), probably influenced by the treatment.

In addition, some potential and, probably, more specific relapse mechanisms could emerge for adult T-ALL patients (e.g. alterations in SMARCA4) that merit further research and validation in a large cohort of adult T-ALL patients. Our data suggest that, at diagnosis, some of the T-ALL leukemias already contain all the genetic variability needed for leukemic cells to evade treatment and promote relapse. This information can serve to delineate more effective and personalized treatment approaches based on the functional abilities of blast cells. Nonetheless, genomic information and clonal evolution characterization, together with transcriptomic and epigenomic data in a large cohort of paired DX–RE samples are required to fully understand relapse in T-ALL.

ACKNOWLEDGMENTS

We thank Santiago Sanchez Sosa, Ricardo Sanchez, Carolina Cañigral, Violeta García, Beatriz Bellosillo, Natalia Estrada, Susana Barrena, Beatriz Soriano, Juana Ciudad, and Caterina Mata for help collecting samples, setting up dPCR experiments, providing immunophenotypic

data, and contributing to the description of the SC methods, respectively. We thank the members of the Hematological Service of Germans Trias i Pujol Hospital. We also thank Gema Fuerte, Ivan Lukic, and Todd Druley to review SC data. In particular, we wish to acknowledge the patients and the Spanish National DNA Bank Carlos III of the University of Salamanca (PT17/0015/0044), integrated within the Spanish National Biobanks Network, for their collaboration (María Pérez and Andrés Montero), the Biobanco la Fe (B.0000723) (Raquel Amigo, José Cervera), and the IGTP/IJC Biobanc (Francesc Solé).

AUTHOR CONTRIBUTIONS

Celia González-Gil performed the experiments, analyzed the data, produced the figures, and helped write the manuscript. Thaysa Lopes prepared libraries and provided technical support to C. González. Mireia Morgades carried out the statistical analyses. Francisco Fuster-Tormo analyzed the sequencing data. Pau Montesinos, Carlos Rodríguez Medina, Lourdes Hermosín, Teresa González-Martínez, María-Paz Queipo, José González-Campos, Pilar Martínez-Sánchez, Marina Diaz-Beya, Rosa Coll, Clara Maluquer, Lurdes Zamora, Teresa Artola, Ferran Vall-Llovera, Mar Tormo, Anna Torrent, Carolina Martínez-Laperche, Cristina Gil-Cortés, Pere Barba, Marta Cervera, Jordi Ribera, Carolina Cañigral, Rosa Ayala, Antonia Cladera, María Carmen Mateos, María Jesús Vidal, Jesús Feliu, Ana Torres, Gemma Azaceta, and María José Calasanz provided clinical data. Anna Bigas and Manel Esteller provided financial support and reagents to the project. Alberto Orfao and Josep Maria Ribera contributed to the study's conceptualization and the data analysis and reviewed the manuscript. Eulalia Genescà designed the study, reviewed the data, and wrote and reviewed the manuscript. All authors have read and approved the manuscript.

CONFLICT OF INTEREST STATEMENT

The authors declare no conflicts of interest.

DATA AVAILABILITY STATEMENT

The datasets used and/or analyzed in the current study are available from the corresponding author on reasonable request (egenesca@carrerasresearch.org).

FUNDING

This project was supported by the AECC (GC16173697BIGA), ISCIII (PI19/01828, PI19/01183, and PI22/01880), co-funded by ERDF/ESF, "A way to make Europe"/"Investing in your future," and CERCA/Generalitat de Catalunya SGR 2021 (ref 00560). Thaysa Lopes was supported by the Leukemia Stiftung (DJCLS 08R/2022).

ORCID

Pau Montesinos  <https://orcid.org/0000-0002-3275-5593>

Anna Torrent  <https://orcid.org/0000-0002-3727-5716>

Josep Maria Ribera  <https://orcid.org/0000-0003-1042-6024>

Eulalia Genescà  <https://orcid.org/0000-0002-5657-4842>

SUPPORTING INFORMATION

Additional supporting information can be found in the online version of this article.

REFERENCES

- Huguet F, Chevret S, Leguay T, et al. Intensified therapy of acute lymphoblastic leukemia in adults: report of the randomized GRAALL-2005 clinical trial. *J Clin Oncol*. 2018;36(24):2514-2523.
- Ribera J-M, Morgades M, Ciudad J, et al. Chemotherapy or allogeneic transplantation in high-risk Philadelphia chromosome-negative adult lymphoblastic leukemia. *Blood*. 2021;137(14):1879-1894.
- Rowntree CJ, Kirkwood AA, Clifton-Hadley L, et al. First analysis of the UKALL14 randomized trial to determine whether the addition of nelarabine to standard chemotherapy improves event free survival in adults with T-cell acute lymphoblastic leukaemia (CRUK/09/006). *Blood*. 2021;138(suppl 1):366.
- Beldjord K, Chevret S, Asnafi V, et al. Oncogenetics and minimal residual disease are independent outcome predictors in adult patients with acute lymphoblastic leukemia. *Blood*. 2014;123(24):3739-3749.
- Petit A, Trinquand A, Chevret S, et al. Oncogenetic mutations combined with MRD improve outcome prediction in pediatric T-cell acute lymphoblastic leukemia. *Blood*. 2018;131(3):289-300.
- Tzoneva G, Perez-Garcia A, Carpenter Z, et al. Activating mutations in the NT5C2 nucleotidase gene drive chemotherapy resistance in relapsed ALL. *Nat Med*. 2013;19(3):368-371.
- Oshima K, Zhao J, Pérez-Durán P, et al. Mutational and functional genetics mapping of chemotherapy resistance mechanisms in relapsed acute lymphoblastic leukemia. *Nat Cancer*. 2020;1(11):1113-1127.
- Alexandrov LB, Nik-Zainal S, Wedge DC, et al. Signatures of mutational processes in human cancer. *Nature*. 2013;500(7463):415-421.
- Li B, Brady SW, Ma X, et al. Therapy-induced mutations drive the genomic landscape of relapsed acute lymphoblastic leukemia. *Blood*. 2020;135(1):41-55.
- Richter-Pechańska P, Kunz JB, Hof J, et al. Identification of a genetically defined ultra-high-risk group in relapsed pediatric T-lymphoblastic leukemia. *Blood Cancer J*. 2017;7(2):e523.
- Sentís I, Gonzalez S, Genescà E, et al. The evolution of relapse of adult T cell acute lymphoblastic leukemia. *Genome Biol*. 2020;21(1):284.
- Alaggio R, Amador C, Anagnostopoulos I, et al. The 5th edition of the World Health Organization Classification of haematolymphoid tumours: lymphoid neoplasms. *Leukemia*. 2022;36(7):1720-1748.
- Ribera J-M, Oriol A, Morgades M, et al. Treatment of high-risk Philadelphia chromosome-negative acute lymphoblastic leukemia in adolescents and adults according to early cytologic response and minimal residual disease after consolidation assessed by flow cytometry: final results of the PETHEMA ALL-AR-03 trial. *J Clin Oncol*. 2014;32(15):1595-1604.
- Ribera JM, García O, Oriol A, et al. Feasibility and results of subtype-oriented protocols in older adults and fit elderly patients with acute lymphoblastic leukemia: results of three prospective parallel trials from the PETHEMA group. *Leuk Res*. 2016;41:12-20.
- Ribera J-M, García O, Chapchap EC, et al. Treatment of frail older adults and elderly patients with Philadelphia Chromosome-negative acute lymphoblastic leukemia: results of a prospective trial with minimal chemotherapy. *Clin Lymphoma Myeloma Leuk*. 2020;20(8):e513-e522.
- González-Gil C, Morgades M, Lopes T, et al. Genomics improves risk stratification of adults with T-cell acute lymphoblastic leukemia enrolled in measurable residual disease-oriented trials. *Haematologica*. 2023;108(4):969-980.
- Uddin M, Thiruvahindrapuram B, Walker S, et al. A high-resolution copy-number variation resource for clinical and population genetics. *Genet Med*. 2015;17(9):747-752.
- Shen R, Seshan VE. FACETS: allele-specific copy number and clonal heterogeneity analysis tool for high-throughput DNA sequencing. *Nucleic Acids Res*. 2016;44(16):e131.
- Zhang X, Su J, Jeong M, et al. DNMT3A and TET2 compete and cooperate to repress lineage-specific transcription factors in hematopoietic stem cells. *Nat Genet*. 2016;48(9):1014-1023.
- Oshima K, Khiabani H, Da Silva-Almeida AC, et al. Mutational landscape, clonal evolution patterns, and role of RAS mutations in relapsed acute lymphoblastic leukemia. *Proc Natl Acad Sci*. 2016;113(40):11306-11311.

21. Ma X, Edmonson M, Yergeau D, et al. Rise and fall of subclones from diagnosis to relapse in pediatric B-acute lymphoblastic leukaemia. *Nat Commun.* 2015;6(1):6604.
22. Malinowska-Ozdowy K, Frech C, Schönegger A, et al. KRAS and CREBBP mutations: a relapse-linked malicious liaison in childhood high hyperdiploid acute lymphoblastic leukemia. *Leukemia.* 2015; 29(8):1656-1667.
23. Zhang J, Ding L, Holmfeldt L, et al. The genetic basis of early T-cell precursor acute lymphoblastic leukaemia. *Nature.* 2012;481(7380): 157-163.
24. Li Y, Buijs-Gladdines JGCAM, Canté-Barrett K, et al. IL-7 receptor mutations and steroid resistance in pediatric T cell acute lymphoblastic leukemia: a genome sequencing study. *PLoS Med.* 2016; 13(12):e1002200.
25. Aries IM, van den Dungen RE, Koudijs MJ, et al. Towards personalized therapy in pediatric acute lymphoblastic leukemia: RAS mutations and prednisolone resistance. *Haematologica.* 2015;100(4):e132-e136.
26. Richard-Carpentier G, Jabbour E, Short NJ, et al. Clinical experience with venetoclax combined with chemotherapy for relapsed or refractory T-cell acute lymphoblastic leukemia. *Clin Lymphoma Myeloma Leuk.* 2020;20(4):212-218.
27. Trinquand A, Tanguy-Schmidt A, Ben AbdelaliAbdelali R, et al. Toward a NOTCH1/FBXW7/RAS/PTEN-based oncogenetic risk classification of adult T-cell acute lymphoblastic leukemia: a Group for Research in Adult Acute Lymphoblastic Leukemia study. *J Clin Oncol.* 2013;31(34):4333-4342.
28. Waanders E, Gu Z, Dobson SM, et al. Mutational landscape and patterns of clonal evolution in relapsed pediatric acute lymphoblastic leukemia. *Blood Cancer Discov.* 2020;1(1):96-111.
29. Richter-Pechańska P, Kunz JB, Rausch T, et al. Pediatric T-ALL type-1 and type-2 relapses develop along distinct pathways of clonal evolution. *Leukemia.* 2022;36(7):1759-1768.
30. Brouwer C, Vogels-Mentink TM, Keizer-Garritsen JJ, et al. Role of 5'-nucleotidase in thiopurine metabolism: enzyme kinetic profile and association with thio-GMP levels in patients with acute lymphoblastic leukemia during 6-mercaptopurine treatment. *Clin Chim Acta Int J Clin Chem.* 2005;361(1-2):95-103.
31. Moriyama T, Liu S, Li J, et al. Mechanisms of NT5C2-mediated thiopurine resistance in acute lymphoblastic leukemia. *Mol Cancer Ther.* 2019;18(10):1887-1895.
32. Meyer JA, Wang J, Hogan LE, et al. Relapse-specific mutations in NT5C2 in childhood acute lymphoblastic leukemia. *Nature Genet.* 2013;45(3):290-294.
33. Dieck CL, Ferrando A. Genetics and mechanisms of NT5C2-driven chemotherapy resistance in relapsed ALL. *Blood.* 2019;133(21): 2263-2268.
34. Stengel A, Kern W, Haferlach T, Meggendorfer M, Fasan A, Haferlach C. The impact of TP53 mutations and TP53 deletions on survival varies between AML, ALL, MDS and CLL: an analysis of 3307 cases. *Leukemia.* 2017;31(3):705-711.
35. Hientz K, Mohr A, Bhakta-Guha D, Efferth T. The role of p53 in cancer drug resistance and targeted chemotherapy. *Oncotarget.* 2016;8(5):8921-8946.
36. Agarwal R, Chan Y-C, Tam CS, et al. Dynamic molecular monitoring reveals that SWI-SNF mutations mediate resistance to ibrutinib plus venetoclax in mantle cell lymphoma. *Nat Med.* 2019;25(1): 119-129.
37. Zhang J, Duan Y, Wu P, et al. Clonal evolution dissection reveals that a high MSI2 level promotes chemoresistance in T-cell acute lymphoblastic leukemia. *Blood.* 2024;143(4):320-335.
38. Turati VA, Guerra-Assunção JA, Potter NE, et al. Chemotherapy induces canalization of cell state in childhood B-cell precursor acute lymphoblastic leukemia. *Nat Cancer.* 2021;2(8):835-852.
39. Spinella J-F, Richer C, Cassart P, Ouimet M, Healy J, Sinnett D. Mutational dynamics of early and late relapsed childhood ALL: rapid clonal expansion and long-term dormancy. *Blood Adv.* 2018;2(3): 177-188.
40. Mullighan CG, Phillips LA, Su X, et al. Genomic analysis of the clonal origins of relapsed acute lymphoblastic leukemia. *Science.* 2008; 322(5906):1377-1380.
41. Kunz JB, Rausch T, Bandapalli OR, et al. Pediatric T-cell lymphoblastic leukemia evolves into relapse by clonal selection, acquisition of mutations and promoter hypomethylation. *Haematologica.* 2015; 100(11):1442-1450.